Tetherless thermobiochemically actuated microgrippers

Timothy G. Leong[a], Christina L. Randall[b], Bryan R. Benson[a], Noy Bassik[a], George M. Stern[a], and David H. Gracias[a,c,1]

Departments of [a]Chemical and Biomolecular Engineering and [c]Chemistry, Johns Hopkins University, 3400 North Charles Street, Baltimore, MD 21218; and [b]Department of Biomedical Engineering, Johns Hopkins University School of Medicine, 720 Rutland Avenue, Baltimore, MD 21205

Edited by James R. Heath, California Institute of Technology, Pasadena, CA, and accepted by the Editorial Board November 25, 2008 (received for review August 5, 2008)

We demonstrate mass-producible, tetherless microgrippers that can be remotely triggered by temperature and chemicals under biologically relevant conditions. The microgrippers use a self-contained actuation response, obviating the need for external tethers in operation. The grippers can be actuated en masse, even while spatially separated. We used the microgrippers to perform diverse functions, such as picking up a bead on a substrate and the removal of cells from tissue embedded at the end of a capillary (an in vitro biopsy).

actuator | biochemical | robotics | thin films

Biological function in nature is often achieved by autonomous organisms and cellular components triggered en masse by relatively benign cues, such as small temperature changes and biochemicals. These cues activate a particular response, even among large populations of spatially separated biological components. Chemically triggered activity is also often highly specific and selective in biological machinery. Additionally, mobility of autonomous biological entities, such as pathogens and cells, enables easy passage through narrow conduits and interstitial spaces.

As a step toward the construction of autonomous microtools, we describe mass-producible, mobile, thermobiochemically actuated microgrippers. The microgrippers can be remotely actuated when exposed to temperatures >40 °C or selected chemicals. The temperature trigger is in the range experienced by the human body at the onset of a moderate-to-high fever, and the chemical triggers include biologically benign reagents, such as cell media. Using these microgrippers, we achieved a diverse set of functions, such as picking up beads off substrates and removing cells from tissue samples.

Conventional microgrippers are usually tethered and actuated by mechanical or electrical signals (1-6). Recently developed actuation mechanisms using pneumatic (7), thermal (8), and electrochemical triggers (9, 10) have also used tethered operation. Because the functional response of currently available microgrippers is usually controlled through external wires or tubes, direct connections need to be made between the gripper and the control unit. These connections restrict device miniaturization and maneuverability. For example, a simple task such as the retrieval of an object from a tube is challenging at the millimeter and submillimeter scale, because tethered microgrippers must be threaded through the tube. Moreover, many of the schemes used to drive actuation in microscale tools use biologically incompatible cues, such as high temperature or nonaqueous media, which limit their utility. There are novel, untethered tools based on shape memory alloys that use low temperature heating, but they have limited mobility and must rely solely on thermal actuation (11, 12). The ability of our gripper design to use biochemical actuation, in addition to thermal actuation, represents a paradigm shift in engineering and suggests a strategy for designing mobile microtools that function in a variety of environments with high specificity and selectivity.

To engineer untethered, mobile grippers, we developed an actuation mechanism that used trilayer joints composed of a polymer and a stressed bimetallic thin film patterned between rigid phalanges (Fig. 1). The microgrippers were fabricated by using conventional multilayer photolithography on a water-soluble sacrificial polyvinyl alcohol layer; this allowed open grippers to be released from the substrate in water. Briefly (detailed in *Methods*), chromium (Cr) and copper (Cu) thin films were thermally evaporated onto the sacrificial layer that had been spin-coated on a silicon wafer. Then, 2 steps of photolithography were performed to fabricate the microgrippers: The first step patterned nickel (Ni) and gold (Au) phalanges, and the second step patterned the polymer trigger and bimetallic (Cr/Cu) layer of the joint. This process enabled large numbers of grippers to be fabricated in a highly parallel and cost-effective manner.

The grippers were structured on a hierarchy of length scales; the films driving actuation were 50–300 nm thick, and the phalanges and joints were tens to hundreds of microns in width and ≈7 μm thick. The entire gripper system was self-contained with a size as small as 700 μm when open and 190 μm when closed. The overall shape of the microgrippers was modeled after biological appendages, such as hands, in which the jointed digits are arranged in different ways around a central palm. For example, the digits in the human hand are arranged in a rotationally asymmetric manner and contain a varying amount of joints; 4 digits contain 3 interphalangeal joints, whereas the fifth (thumb) only has 2 (13). In our gripper designs, we varied the number and arrangement of digits around the palm (Fig. 2 *A* and *B*), the shape of the central polygonal palm (Fig. 2 *C–E*), and the number of interphalangeal joints (Fig. 2 *F–H*). We also incorporated tapered distal phalanges (emulating sharp nails or claws) to enable extrication of cells and tissue in our experiments.

We observed that an asymmetric arrangement of digits left a large gap within the closed gripper (Fig. 2*A*), whereas grippers with a symmetrical arrangement of digits (Fig. 2*B*) retained objects more effectively. We found that grippers with fewer digits were more likely to close properly (higher yield), because a smaller number of joints needed to flex. However, grippers with more digits had an increased defect tolerance and were still able to hold on to objects despite a few defective joints. In our study, we found that grippers with 6 rotationally symmetric digits achieved a sufficient balance between yield and defect tolerance.

Author contributions: T.G.L., C.L.R., B.R.B., and D.H.G. designed research; T.G.L., C.L.R., B.R.B., and G.M.S. performed research; N.B. and G.M.S. contributed new reagents/analytic tools; T.G.L., C.L.R., N.B., G.M.S., and D.H.G. analyzed data; and T.G.L., C.L.R., B.R.B., N.B., G.M.S., and D.H.G. wrote the paper.

The authors declare no conflict of interest.

This article is a PNAS Direct Submission. J.R.H. is a guest editor invited by the Editorial Board.

[1]To whom correspondence should be addressed at: 3400 North Charles Street, 125 Maryland Hall, Baltimore, MD 21218. E-mail: dgracias@jhu.edu.

This article contains supporting information online at www.pnas.org/cgi/content/full/0807698106/DCSupplemental.

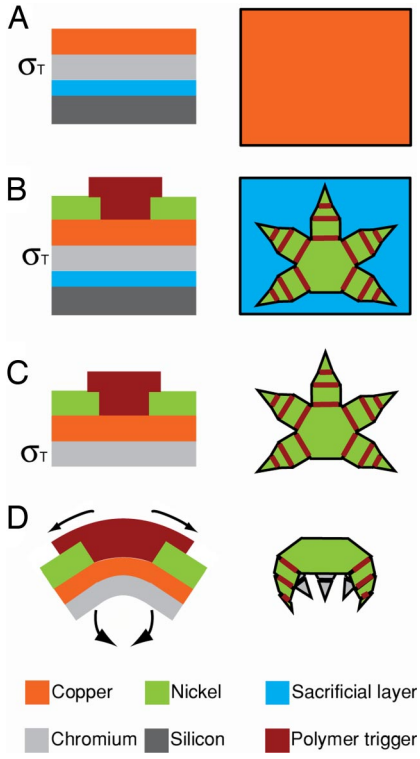

Fig. 1. Schematic diagram depicting side and top views of the key steps in the fabrication and operation of the microgripper trilayer joints. (*A*) The bimetallic joint component (orange and light gray) was evaporated above the sacrificial layer (blue) and silicon (dark gray) substrate. The Cr layer (light gray) developed residual tensile stress during evaporation, denoted by σ_T. (*B*) The Ni phalange (green) and the polymer trigger layer (red) were then patterned above the bimetallic layer. (*C*) The sacrificial layer was dissolved to release the microgripper from the substrate in a planar, open configuration. (*D*) When heated or exposed to selected chemicals, mechanical property changes in the polymer trigger allowed the stressed bimetallic layer to flex.

The microgripper digits were inspired by the dicondylic joints of arthropods (14) and designed as a series of rigid Ni and Au phalanges, interconnected by hybrid organic–inorganic flexible trilayer joints. The joints consisted of 2 components: a Cr/Cu thin film bilayer and a polymer trigger (Fig. 1). When actuated, grippers with 2-jointed digits (Fig. 2*F*) formed right prisms, whereas grippers with 3-jointed digits (Fig. 2*G*) curled into themselves, such that the distal and proximal phalanges were parallel. We observed that grippers with 3-jointed digits held onto beads tighter than those with 2-jointed digits. This increased grip was because the extra joint was unable to relieve all of its residual stress; hence, the distal phalange pressed against the captured bead that impeded its motion (Fig. 2*H*). Thus, for capture and retrieval experiments, we used rotationally symmetric, 6-digit, 3-jointed grippers.

The metallic bilayer of the joints was crucial to the operation of the gripper. We fabricated a stressed Cr thin film by thermal evaporation (15-18) and subsequently evaporated a minimally stressed Cu film to form the bilayer. The flexing of the bimetallic joints (to close the gripper) was driven by the release of residual tensile stress within the Cr thin film, and similar bending behavior of stressed thin films has been previously observed (8, 19-24). We found both experimentally and theoretically (Fig. 3), that a bimetallic layer composed of 50-nm Cr and 200- to 250-nm Cu reproducibly resulted in joint flexing angles of ≈90°.

Microgrippers with joints composed of only the metallic bilayer closed spontaneously when released from the substrate. However, the addition of the polymer layer to form trilayer joints

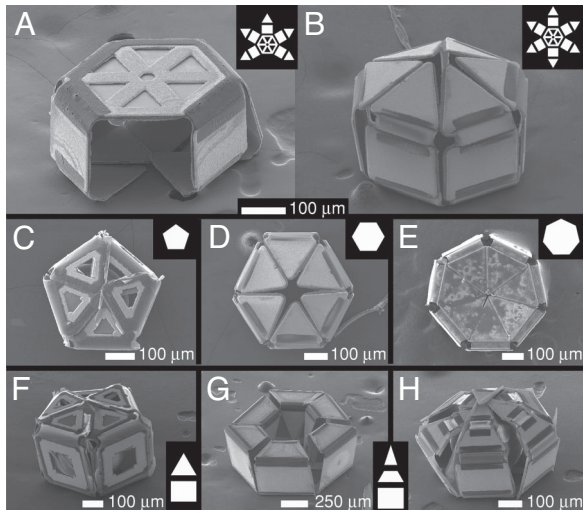

Fig. 2. Scanning electron microscope images highlighting variability in rotational symmetry, number of digits and palm shape, and number of joints per digit. (*A* and *B*) Closed microgrippers with a rotationally asymmetric (*A*) and symmetric (*B*) arrangement of digits around the central palm. Note the gap in gripper *A* that resulted because of the asymmetry. The *Insets* depict the layout of the gripper when open. (*C*–*E*) Closed grippers with pentagonal (*C*), hexagonal (*D*), and heptagonal (*E*) palms and a symmetric arrangement of digits. (*F*–*H*) Closed grippers with 2-jointed digits (*F*) and 3-jointed digits (*G* and *H*). The *Insets* depict the open configuration of each digit. (*G*) Empty gripper with 3 digits closed such that the distal phalange is parallel to the proximal phalange. (*H*) Gripper closed around a bead. When the bead was captured, the distal phalanges could not flex completely and pushed against the bead.

enabled triggered control over the closing of the gripper. The polymer layer also increased the mechanical strength of the gripper. In our present study, we used a commercial photoresist in which the polymer is a cresol novolak resin (details in *Methods*). Cresol novolak resin-based photoresists that have not been hard-baked experience a thermal transition point in the range of 40–60 °C (25-27). We verified this transition on our processed polymer films with differential scanning calorimetry [details in supporting information (SI) Fig. S1]. When heated, the mechanical properties of the polymer were altered, and grippers heated >40 °C closed. The grippers could also be actuated by chemicals that altered the mechanical properties of the polymer (through processes such as softening or chemical degradation). Chemicals that dissolved or caused delamination of the polymer layer from the joint also triggered the closing of the gripper. Before either thermal or chemical actuation, the

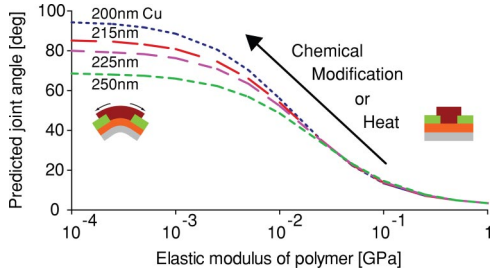

Fig. 3. Dependence of the multilayer joint angle on thin film parameters. Predicted joint angles resulting from a change in polymer elasticity for various Cu thicknesses in the range of 200–250 nm (Cr was kept constant at 50 nm). The joint angles were predicted from a multilayer thin film model (details in *SI Text*). The theoretical calculation reflects the change in the polymer elastic modulus and the resulting joint angle as the polymer layer of the joint is triggered with heat or chemicals.

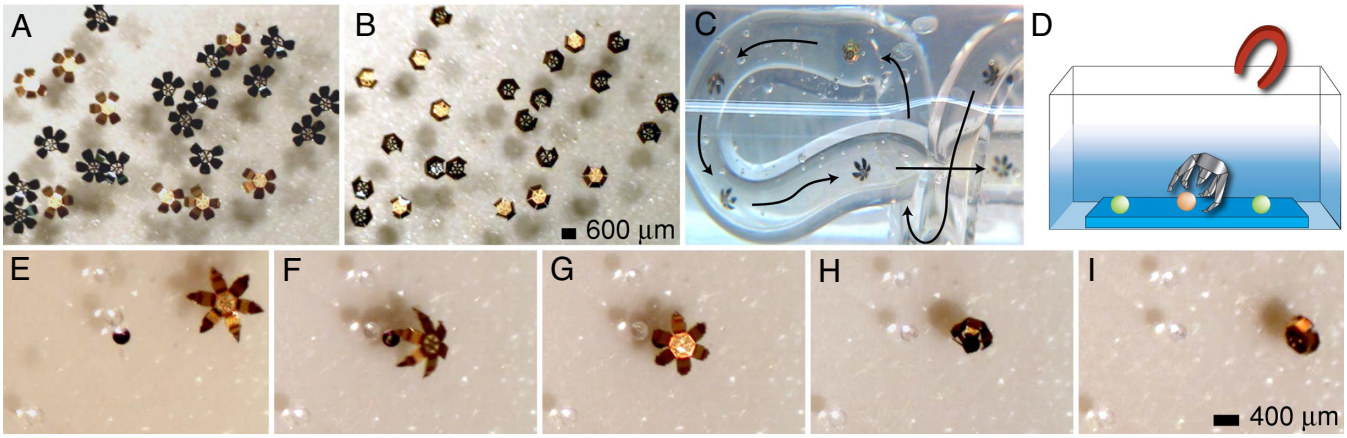

Fig. 4. Thermally triggered actuation, magnetic manipulation, and bead capture. (*A* and *B*) Optical images of 23 grippers (face-up and face-down) triggered to close en masse by heating. (*C*) Overlaid movie sequence (Movie S1) showing the remote-controlled manipulation of a mobile gripper in a coiled tube. (*D*) Schematic diagram depicting remote, magnetically directed movement and capture of a bead on a substrate. (*E–I*) Optical microscopy sequence showing the remote-controlled, thermally triggered capture of a dyed bead (275 μm) from among several clear beads.

polymer was stiff and well-adhered enough to the underlying Cr/Cu bilayer to prevent the spontaneous flexing of the individual joints, thereby keeping the gripper flat and open. When the mechanical properties of the polymer were altered (by thermal or chemical cues), the Cr/Cu bilayer beneath was allowed to flex, resulting in the closure of the gripper. Thus, trilayer-jointed microgrippers remained open after release from the fabrication substrates (Fig. 4*A*) and closed en masse (Fig. 4*B*) only when triggered. A variety of chemicals, including organic solvents (e.g., acetone, alcohols, *N*-methylpyrrolidone, and dimethyl sulfoxide) and caustics (e.g., sodium and potassium hydroxides) can chemically actuate the grippers. For biological applications, we screened a variety of biochemicals and observed that actuation was also possible with triggers such as L-glutamine, glucose, and L929 media. As compared with caustics and organic solvents that tended to dissolve the polymeric trigger, we observed that the biochemicals attacked the polymer and polymer–Cu interface, resulting in cracking and decreased adhesion to the underlying bilayer.

Regardless of the actuation method, we observed that any mechanical property changes (both elastic and plastic) that occurred within the polymer during actuation were important. To understand the correlation between elastic mechanical property changes in the polymer and the flexing of the joints, we applied a model using published equations that predict the curvature of multilayer films (19, 28, 29). The equations captured the effect of elastic deformations in a plane strain condition and were used mainly to gain insight into the actuation mechanism. For a given joint length and width composed of elastically isotropic thin films, the product of residual stress and thickness of each film dictated the final flex angle of the joint. Using a KLA-Tencor Flexus FLP2904 wafer curvature thin film stress device, we first determined that 50-nm films of Cr evaporated by our equipment (thickness measured by using a quartz crystal microbalance integrated within the evaporator) directly onto silicon wafers had residual stresses of ≈1 GPa and that 200–250 nm of Cu had tensile residual stresses of ≈0.04–0.08 GPa, respectively; these values are consistent with those reported in literature (17). Taking the literature values for elastic moduli of Cr and Cu films to be 144 GPa (30) and 130 GPa (31), the model (details in *SI Text*) predicted a bend angle of 95°–70° for a Cr/Cu bilayer (with no polymer) composed of a range of Cu thicknesses between 200 and 250 nm, respectively (Fig. 3). The predicted angles were consistent with experimental observations for joint flexing after complete dissolution of the polymer layer. When the thin film bending model was extended to 3 layers, accounting for the presence of an untriggered polymer component, the model predicted very slight bending (on the order of a few degrees) when the modulus of the polymer was ≈0.5 GPa. This matched the observation that grippers with trilayer joints remained flat upon liftoff at room temperature. The model suggested that the elastic modulus of the polymer needed to be decreased below ≈10 MPa for the joint to flex significantly (Fig. 3). A trilayer joint with a polymer trigger having an elastic modulus reduced to ≈800 kPa achieved a flex angle that was 95% of that produced by a bare Cr/Cu bilayer. This modulus falls within the range of soft materials, such as silicone dental impression material (≈500 kPa) (32). Thus, any process that alters the polymeric trigger to decrease its elastic modulus to within this kPa-to-MPa range can cause actuation of the gripper. It should be noted that any plastic deformation of the polymer (which also likely occurs during actuation) by biochemical or thermal triggers was beyond the scope of the model.

In addition to characterizing the design, we performed application-oriented experiments to highlight the utility of the microgrippers. Because the grippers were untethered and fabricated with Ni (a ferromagnetic material) phalanges, they could be precisely manipulated by using a magnet from distances as far away as 10 cm. As opposed to tethered grippers, the mobile microgrippers were easily moved through coiled tubes (Fig. 4*C* and Movie S1). Additionally, multiple microgrippers could be moved simultaneously. However, if they were brought too close, the ferromagnetic grippers attracted each other and became entangled; thus, for precision applications, they were used individually. By enabling remote control of movement and by using thermal triggering of gripper closure, it was possible to perform spatiotemporally controlled capture and retrieval of glass beads (Fig. 4 *D–I*). Shown in Fig. 4 *E–I* is a gripper that was remotely manipulated to selectively retrieve a dyed bead among numerous colorless beads in water (see also Fig. S2). The gripper was moved over the bead, and the temperature of the solution was increased to trigger closing. The gripper firmly grasped the bead and was remotely manipulated while carrying the bead within its grasp. This process was highly reproducible, even with smaller grippers (Movie S2).

Because the microgrippers could be actuated in biologically compatible, aqueous environments, we used them to capture clusters of live L929 fibroblast cells from dense cell masses deposited at the end of 1.5-mm-diameter capillary tubes. Shown in Fig. 5 *A–C* and Movie S3 is a gripper that was remotely guided

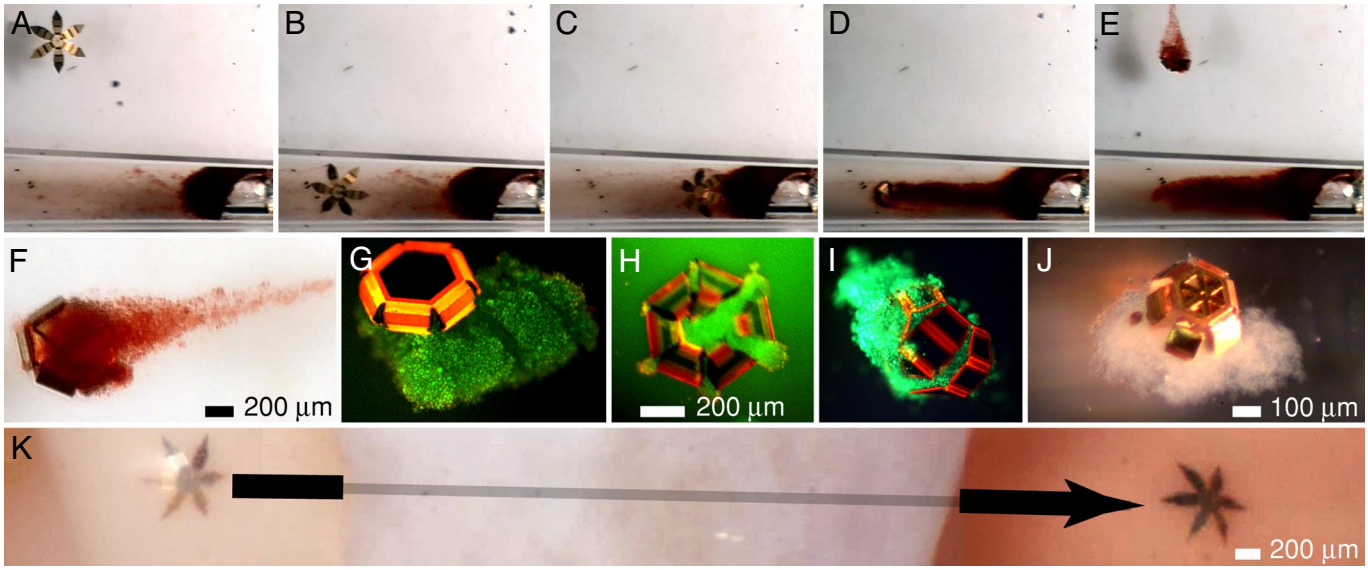

Fig. 5. Thermally and biochemically triggered cell capture. (*A–E*) Optical microscopy sequence showing the thermally triggered capture and retrieval of Neutral red-stained cells from a cell culture mass at the end of a 1.5-mm-diameter tube (Movie S3). (*F*) Zoomed detail of the microgripper with the cells captured in *A–E* demonstrating viability (red). (*G*) Fluorescent micrograph demonstrating viability of thermally captured LIVE/DEAD stained cells. Note that the photopatternable polymer in the joints fluoresces red under UV excitation. (*H*) Fluorescent micrograph with viable cells (green) captured by using a thermal trigger and incubated for 72 h afterward. (*I*) Fluorescent micrograph of viable cells captured by using a biochemical trigger to actuate the gripper. (*J*) Optical image of a microgripper with captured cells from a sample of a bovine bladder. (*K*) Overlaid optical micrograph sequence depicting the traversing of a gripper from left to right through an orifice in a bovine bladder tissue sample.

into a capillary tube and thermally triggered to grasp a portion of a living cell mass stained with Neutral red (a red stain that accumulates in lysosomes after diffusing through the cell membrane of viable cells). The microgripper was then guided out of the capillary with the captured cells in its grasp (Fig. 5 *D* and *E*). The cells were still viable, as indicated by their red color, and the cluster of cells after retrieval can be seen in Fig. 5*F*. The experiment was repeated numerous times with LIVE/DEAD stain to further demonstrate cell viability after thermally triggered capture (Fig. 5*G*). After retrieval, we placed cell-loaded grippers into media and incubated them for 72 h; the cells were still viable (Fig. 5*H*), signifying that the materials used in the fabrication of the grippers and the capture and retrieval processes were not harmful to the cells. The viability of the captured cells after incubation provides evidence that the grippers could be used as biological storage devices until the samples are ready to be analyzed.

In addition to thermally triggering the grippers, we used biochemical-triggered actuation to capture live cells. We observed that grippers closed to some degree in a variety of biochemicals, including aqueous solutions of glucose, trypsin, and L929 cell media (detailed list in *SI*). It is important to note that the time required to close the microgrippers with biochemical triggers was longer than that needed with thermal or caustic/solvent-based actuation. We believe that biochemical actuation occurs as a result of a chemical attack of the polymer–Cu interface, a process that takes longer and results in decreased adhesion of the polymer. Based on the results from our biochemical screening and the fact we were using L929 cells, we chose to use L929 cell media as a biocompatible trigger. Grippers were placed into centrifuged solutions containing L929 cells and L929 media and then placed into an incubator to sustain the cells. It is important to note that the grippers partially closed at room temperature when exposed to L929 media but further closed under the incubator conditions used to maintain the cells (details in Table S1). After 30 min, the grippers closed around cells, and they were imaged after 4 h. Rather than imaging the grippers immediately, waiting 4 h allowed us to determine whether any apoptotic (as opposed to necrotic) cell death had occurred. Fig. 5*I* features a fluorescent micrograph of a gripper closed around live (green) L929 cells after 4 h in L929 media.

To explore the utility of the gripper in microsurgical applications, we performed an in vitro biopsy on a tissue sample from a bovine bladder (Fig. 5*J*) loaded into a 1.5-mm glass capillary tube (see also Fig. S3). This experiment necessitated the use of the magnet to rotate the gripper such that the claw phalanges could cut through the connective tissue and extricate the cells. This experiment demonstrated that even though the grippers had nanomicroscale actuation joints, they were strong enough to perform an in vitro tissue biopsy.

Also, we magnetically manipulated a microgripper in different regions of whole bovine bladder tissue, including both rough and smooth areas. It was observed that the claw would become adhered and immobile when manipulated across the rough tissue, because the claw phalanges became entangled with the tissue. However, the gripper could eventually be dislodged with continued magnetic manipulation. On smooth tissue, it was observed that the claw could be easily manipulated. Fig. 5*K* shows a gripper that was manipulated through an orifice in the bladder tissue.

Once closed, the contents of the grippers could be retrieved in a biocompatible manner by mechanical disruption. Beads retrieved from the gripper were not damaged, and retrieved cells were viable (Figs. S2 and S4). After retrieving the microgrippers with captured cells, they were mechanically agitated by using a variety of methods (including force applied via Pasteur pipette tip, prying open with 22-G syringe tips, and vortexing) to release the cells. Vortexing also provided a way of releasing the cells and leaving the microgripper intact. Vortexing dispersed the cells, making them hard to find and image, but the cells could be centrifuged and collected for further testing. To release captured clumps of cells without dispersing them, we used either a Pasteur pipette or syringe tips to open the grippers; however, this method typically damaged the microgrippers. Ideally, it would be pos-

sible to both close and open the grippers under biological conditions in a reversible manner; we have yet to demonstrate this feature with tetherless grippers. Presently, our grippers function only in single-use capture applications, such as those demonstrated (e.g., capture and retrieval of objects and biopsies). For applications such as biopsies, the lack of reusability is not a concern, because the grippers are fabricated en masse and are inexpensive. However, other combinations need to be explored to enhance the functionality of microgrippers by enabling features such as multiuse, reversible operation and triggering based on more specific biochemical cues. Actuation based on highly specific biochemical triggers is attractive for autonomous function, and these cues are widely observed in nature, e.g., receptor–ligand binding-triggered endocytosis. In the present case, our grippers are actuated by a wide range of biochemicals, and there exists the possibility for falsely triggered actuation due to a nonspecific response.

Regarding size, our closed grippers are ≈5–20 times larger than mammalian cells; smaller grippers will need to be constructed for single-cell capture studies. This decrease in size will require a redesign of the joint to incorporate thin films that experience higher stress (as compared with the particular demonstrated combination of Cr/Cu) that can achieve tighter radii of curvature. Additionally, for smaller grippers, advanced lithographic schemes such as electron beam lithography may be needed to pattern any submicron-scale features.

In summary, we have developed microgrippers with features widely observed in microscale biological components, namely mobility and mass-actuation based on biologically benign cues. We envision the use of these mass-producible, mobile grippers in the capture and retrieval of objects from hard-to-reach places, such as within tubes and capillaries of microfluidic devices, and possibly even in microsurgical procedures. At the present time, internal biopsies are performed through the use of tethered microsurgical tools. It is difficult to manipulate tethered systems around corners and in coiled geometries; hence, we believe our mobile grippers may allow for the development of minimally invasive microsurgical tools. However, regarding in vivo microsurgical procedures, several challenges arise. Our microgrippers represent an image-guided platform, and techniques such as magnetic resonance imaging or computed tomography will be needed for in vivo guidance. One highlight here is that our microgrippers are metallic; hence, these structures can be easily imaged by using magnetic resonance techniques (33) and specifically wirelessly heated by using electromagnetic fields (34). Another possible complication is that the grippers may become lodged in tissue before reaching the target destination, though we have observed, remarkably, that the grippers can be moved over large distances over certain types of tissue without becoming entangled (Fig. 5*K*). Guidance and actuation on different tissue types, as well as under fluid environments that experience high shear, need to be investigated. Nevertheless, it should be noted that the microgrippers represent a step toward the development of biocompatible, minimally invasive, autonomous microtools. Finally, the principles used in the design of the gripper highlight the utility of thin film actuation and self-assembly as attractive paradigms for enabling mass-producible, mass-actuating, and miniaturized machine-based function in human-engineered systems.

Methods

For a complete list of biochemicals commonly used with biological experiments, see Table S1.

Fabrication of the Microgrippers. All microgrippers were constructed as flat 2D structures on silicon substrates by using standard photolithographic techniques (24). A sacrificial layer (≈5 μm) of poly(vinyl alcohol) (PVA, $M_w = 6{,}000$; Polysciences) was first spun onto a silicon wafer and baked for 12 h at 115 °C. Then, 50-nm chromium (Cr) and 200- to 250-nm copper (Cu) thin films were thermally evaporated onto the substrate. Microposit SC 1827 (Microchem) was spincoated onto the wafer and patterned with a photomask (Fineline Imaging) containing the phalange features. The photopatternable polymer was developed and the microgripper phalanges electrodeposited with nickel (6 μm) and gold (500 nm) by using commercial electrolytic solutions (Technic, Inc.). The gold capping layer enhanced wet-etch resistance and biocompatibility of the microgrippers. A second photolithographic step patterned the trilayer joints, and the exposed surrounding Cu and Cr seed layers were etched by using commercial etchants, APS-100 and CRE-473 (Technic, Inc.), respectively. The open microgrippers were released from the substrate by immersion of the silicon wafer in water, which dissolved the sacrificial PVA layer.

Thermal Triggering of the Microgrippers. Grippers were typically placed into a dish of water and heated by using a hotplate above ≈40 °C to trigger the closing of the microgripper. Alternatively, a faster method of heating was performed by using a heat gun (Black & Decker), but the temperature was difficult to regulate, leading to the possibility of causing damage to the cells.

Thermally Triggered Capture and Retrieval of a Glass Bead: Experimental Details of the Demonstrations Shown in Fig. 4 *E–I* and Movie S2. One dyed and numerous clear ≈275-μm glass microspheres (Polysciences) were placed into a glass dish containing water. A microgripper (375-μm diameter when closed) was placed into the dish by using a large tipped pipette and guided with a magnet from afar, over to the dark bead. Once the gripper was in place, the dish was heated above ≈40 °C by using a hotplate to trigger the closing of the microgripper. After the dyed bead was captured, the microgripper was moved away with the magnet. This process was repeated in Movie S2 with ≈100-μm glass microspheres (Polysciences) and a smaller microgripper (190 μm when closed).

L929 Cell Preparation and Staining with Neutral Red. Mouse fibroblast cells (L929; Sigma) were cultured and maintained following standard cell culture protocols. Briefly, the cells were cultured in 75-cm^2 culture flasks in 85% Minimum Essential Medium Eagles containing L-glutamine and sodium bicarbonate with 10% horse serum and supplemented with MEM nonessential amino acids and sodium pyruvate. The cells were maintained in an incubator set to 37 °C with a water-saturated 5% CO_2 atmosphere. The cells were trypsinized and transferred to an Eppendorf tube containing a 1:10 concentration of Neutral red (Invitrogen) dye (which stains live cells red) in L929 media and allowed to uptake the dye for a period of 45–60 min.

L929 Cell Preparation and Staining with LIVE/DEAD Stain. L929 mouse fibroblast cells (Sigma) were cultured and maintained following standard cell culture protocols. The cells were trypsinized, resuspended in 4 mL of L929 media, and transferred to 15-mL conical tubes and subsequently centrifuged at 377 × *g* for 5 min. This resulted in the formation of a dense cell mass. The cells were stained either before or after capture with the LIVE/DEAD 2-color fluorescence stain (Invitrogen). The Calcein AM component stains live cells green and ethidium homodimer-1 stains dead or damaged cells red.

Thermally Triggered Capture of Live Cells: Experimental Details of the Demonstration Shown in Fig. 5 *A–F*. A glass capillary tube ≈1.5 mm in diameter was plugged at one end with a polydimethylsiloxane stopper and subsequently loaded with the stained cells. The capillary tube with the cells was centrifuged at 42 × *g* for 5 min to produce a dense cell mass at the plugged end. The capillary and a released microgripper were then placed into PBS, and the microgripper was remotely guided by using a magnet to enter the capillary from the accessible end to approach the cell mass. When the microgripper was next to the cell mass, the solution was heated briefly (<1–2 min) on a hotplate and the microgripper closed around the cells. Upon closing, the microgripper containing a sampling of cells was magnetically guided out of the capillary back to the original starting position.

Retrieval of Viable Cells from the Microgripper. After retrieving microgrippers that had captured cells, the grippers were mechanically disrupted by applying force via Pasteur pipette tip or prying open with 22-G syringe tips. The grippers and cells were then stained with LIVE/DEAD stain and imaged by using fluorescent microscopy.

Thermally Triggered Capture of Cells for Culture: Experimental Details of the Demonstration Shown in Fig. 5*H*. Centrifuged L929 cells were loaded into a vertical 1.5-mm diameter glass capillary containing L929 cell media and allowed

to settle due to gravity as a large cell mass. The loaded capillary was placed into a Petri dish filled with L929 cell media and a microgripper. The microgripper was magnetically manipulated into the capillary and captured a clump of the cells upon heating. This process was easily performed and successfully repeated >2 dozen times. Upon retrieval from the capillary, the microgripper loaded with captured fibroblast cells was placed into new media and incubated for 72 h. LIVE/DEAD stain was applied to verify the viability of the cells.

Biochemical-Triggered Capture of Cells: Experimental Details of the Demonstration Shown in Fig. 5*I*. Two separate tests where devised to capture live cells by using biochemically induced actuation. In the first test, L929 cells were centrifuged, and half of the supernatant was added to a small plastic Petri dish containing 5 mL of L929 media. Two grippers were then added to the Petri dish, and the dish was placed into an incubator at 37 °C. In the second test, cells where centrifuged in L929 media, and 2 grippers were added directly to the centrifuge tube, where they settled into the cell mass. The test tube was incubated at 37 °C. The grippers were separated from the cells by using a magnet and imaged after 4 h.

In Vitro Biopsy of a Bovine Bladder: Experimental Details of the Demonstration Shown in Fig. 5*J* and Fig. S3. A core sample of bovine bladder tissue (Innovative Research) was taken with a 1.5-mm-diameter glass capillary, thus plugging the end of the capillary tube. The experiment was performed in a manner similar to the cell-capture experiments. A microgripper was guided into the capillary and heated to close around a clump of the bladder tissue. To retrieve the microgripper with a sample, the magnet used for guidance was rotated to spin the microgripper, allowing the nail phalanges to cut the connective tissue, extricate the cell mass, and become free of the tissue. After cutting through, the microgripper was guided out of the capillary and imaged with the captured bladder cells.

Manipulation of a Gripper in Bovine Bladder Tissue (Fig. 5*K*). Bovine bladder tissue was placed into a large Petri dish filled with phosphate buffer saline. A gripper was placed into the solution on the bladder tissue. We manipulated the gripper through an opening in the tissue where blind manipulation was required.

ACKNOWLEDGMENTS. We acknowledge the illustration contributions from Aasiyeh Zarafshar and Anum Azam and differential scanning calorimetry assistance from Kedar D. Deshmukh and Howard E. Katz. This material is based in part on work supported by the National Science Foundation under Grants CMMI-0448816 and DMR05-20491; by the National Institutes of Health under Grant 1R21EB007487-01A1; and by the Dreyfus and the Beckman Foundations. Any opinions, findings, and conclusions or recommendations expressed in this material are those of the authors and do not necessarily reflect the views of the funding agencies.

1. Angelo JA (2006) *Robotics, A Reference Guide to a New Technology* (Greenwood Press, Westport, CT).
2. Madden JD (2007) Mobile robots: Motor challenges and materials solutions. *Science* 318:1094–1097.
3. Cecil J, Powell D, Vasquez D (2007) Assembly and manipulation of micro devices—A state of the art survey. *Robot Comput Integrated Manufacturing* 23:580–588.
4. Kim CJ, Pisano AP, Muller RS, Lim MG (1992) Polysilicon microgripper. *Sensors Actuators A Phys* 33:221–227.
5. Pister KSJ, Judy MW, Burgett SR, Fearing RS (1992) Microfabricated hinges. *Sensors Actuators A Phys* 33:249–256.
6. Lee AP, *et al.* (1996) A practical microgripper by fine alignment, eutectic bonding and SMA actuation. *Sensors Actuators A Phys* 54:755–759.
7. Lu YW, Kim CJ (2006) Microhand for biological applications. *Appl Phys Lett* 89:1641011–1641013.
8. Luo JK, *et al.* (2006) Modelling and fabrication of low operation temperature microcages with a polymer/metal/DLC trilayer structure. *Sensors Actuators A Phys* 132:346–353.
9. Jager EWH, Inganäs O, Lundström I (2000) Microrobots for micrometer-size objects in aqueous media: Potential tools for single-cell manipulation. *Science* 288:2335–2338.
10. Shahinpoor M, Bar-Cohen Y, Simpson JO, Smith J (1998) Ionic polymer-metal composites (IPMCs) as biomimetic sensors, actuators and artificial muscles—A review. *Smart Mater Struct* 7:R15–R30.
11. Buckley PR, *et al.* (2006) Inductively heated shape memory polymer for the magnetic actuation of medical devices. *IEEE T Biomed Eng* 53:2075–2083.
12. Small W, *et al.* (2007) Prototype fabrication and preliminary in vitro testing of a shape memory endovascular thrombectomy device. *IEEE T Biomed Eng* 54:1657–1666.
13. Flatt AE (2002) Our thumbs. *Proc Baylor Univ Med Center* 15:380–387.
14. Chapman RF (1982) *The Insects: Structure and Function* (Harvard Univ Press, Cambridge, MA).
15. Abermann R, Martinz HP (1984) Internal stress and structure of evaporated chromium and MgF2 films and their dependence on substrate temperature. *Thin Solid Films* 115:185–194.
16. Hoffman RW, Daniels RD, Crittenden EC, Jr (1954) The cause of stress in evaporated metal films. *Proc Phys Soc London B* 67:497–500.
17. Klokholm E, Berry BS (1968) Intrinsic stress in evaporated metal films. *J Electrochem Soc* 115:823–826.
18. Thornton JA, Hoffman DW (1989) Stress-related effects in thin films. *Thin Solid Films* 171:5–31.
19. Arora WJ, Nichol AJ, Smith HI, Barbastathis G (2006) Membrane folding to achieve three-dimensional nanostructures: Nanopatterned silicon nitride folded with stressed chromium hinges. *Appl Phys Lett* 88:0531081–0531083.
20. Chua CL, Fork DK, Van Schuylenbergh K, Lu JP (2003) Out-of-plane high-Q inductors on low-resistance silicon. *J Microelectromech Soc* 12:989–995.
21. Moiseeva E, Senousy YM, McNamara S, Harnett CK (2007) Single-mask microfabrication of three-dimensional objects from strained bimorphs. *J Micromech Microeng* 17:N63–N68.
22. Schmidt OG, Eberl K (2001) Thin solid films roll up into nanotubes. *Nature* 410:168.
23. Doerner MF, Nix WD (1988) Stresses and deformation processes in thin films on substrates. *CRC CR Rev Sol State* 14:225–268.
24. Leong TG, Benson BR, Call EK, Gracias DH (2008) Thin film stress-driven self-folding of microstructured containers. *Small* 4:1605–1609.
25. Morton SL, Degertekin FL, Khuri-Yakub BT (1999) Ultrasonic sensor for photoresist process monitoring. *IEEE Transact Semiconductor Manufacturing* 12:332–339.
26. Gogolides E, Tegou E, Beltsios K, Papadokostaki, Hatzakis M (1996) Thermal and mechanical analysis of photoresist and silylated photoresist films: Application to AZ 5214^{TM}. *Microelectron Eng* 30:267–270.
27. Paniez PJ, Chollet J-PE, Pons MJ (1993) Thermal properties of state of the art novolak-diazonaphtoquinone systems: Differences between bulk and film properties. *Proc SPIE* 1925:614–625.
28. Nikishkov GP (2003) Curvature estimation for multilayer hinged structures with initial strains. *J Appl Phys* 94:5333–5336.
29. Bassik NB, Stern GM, Gracias DH (2008) Patterning thin film mechanical properties to drive assembly of complex 3D structures. *Adv Mater* 20:4760–4764.
30. Qi ZQ, Meletis EI (2005) Mechanical and tribological behavior of nanocomposite multilayered Cr/a-C thin films. *Thin Solid Films* 479:174–181.
31. Freund LB, Suresh S (2003) *Thin film materials: Stress, Defect Formation, and Surface Evolution* (Cambridge Univ Press, Cambridge, UK).
32. Jamani KD, Harrington E, Wilson HJ (1989) Rigidity of elastomeric impression materials. *J Oral Rehab* 16:241–248.
33. Gimi B, *et al.* (2005) Self-assembled three dimensional radio frequency (RF) shielded containers for cell encapsulation. *Biomed Microdev* 7:341–345.
34. Ye HK, *et al.* (2007) Remote radio-frequency controlled nanoliter chemistry and chemical delivery on substrates. *Angew Chem Int Ed* 46:4991–4994.